Parametrisation of interdigit comb capacitor for dielectric impedance spectroscopy

F. Starzyk *

Institute of Physics, Cracow University of Technology,
ul. Podchorążych 1, 30-084 Kraków, Poland
* Corresponding author: E-mail address: fstarzyk@ifpk.pk.edu.pl

ABSTRACT

Purpose: The purpose of this paper was to collect full description of interdigit capacitor (IDC) used in interdigit dielectrometry and to point out on the way how it should be applied in practice.

Design/methodology/approach: The full graphical representation of IDC geometry and its description was demonstrated and described. Capacity of IDC and electric potential distribution as well as charge density distribution on flat comb electrodes were demonstrated.

Findings: Though the analytical formulas of effective IDC capacity and potential distribution are complicated, the practical application of IDC in dielectric measurements is much simpler than those of flat or cylindrical capacitors.

Research limitations/implications: Practical limitations were formulated and specified together with their meanings.

Practical implications: Universality of measuring procedure with IDC application was pointed out and completed.

Originality/value: Complete description of IDC parameters will make easier for potential investigator from many scientific disciplines to see how one have to understand and apply in practice IDC dielectrometry technique as well as potentially make the IDC parameter optimal for given application.

Keywords: Electrical properties; Interdigit comb capacitor; Impedance spectroscopy

## PROPERTIES

1. Introduction

Interdigital dielectrometry applies plane interdigital electrodes (or interdigital capacitors (IDC)) for measurements of frequency dependent dielectric properties of polymeric layers [1], liquids [2], granular and micro-granular matter [3-6]. The values of physical variables sensitive to dielectric properties changes can be monitored. These involves changes in moisture, density porosity, chemical vapours and many more. IDC technique is introduced in physical, chemical, biochemical and medical investigations. The artificial nose [7] and in food technology [8, 9] can close this specification but it is fare from being complete.

Traditional flat capacitor model as well as cylindrical one is well known but model of IDC, the electric field distribution, the spatial distribution of electric potential and other specific features of IDC are rather weakly described and known among scientist, physicians and technologist dealing with material technology and investigations. It seems that number of practical applications of IDC measurements and tests will be increasing rapidly in the nearest future. Thus, any attempt to summarize model approach to IDC is or should be desired.

2. Geometry of plane interdigital capacitor

Schematic layout of interdigit capacitor geometry and its parameters are demonstrated in the Fig. 1. Typical L and D values equal about 10mm or less. The substrate thickness is of 2mm in fused quartz case. The (x, y, z) coordinate system orientation is also shown. The metallic comb electrodes are made of Au, Pt, ITO, Cr. In most cases flat electrodes approximation (g « w) is valid (Fig. 2). Cross-section A-A layout from Fig.1 with electric field strength lines and iso-lines of electric potential created by comb electrodes above the plain and within substrate material is demonstrated.
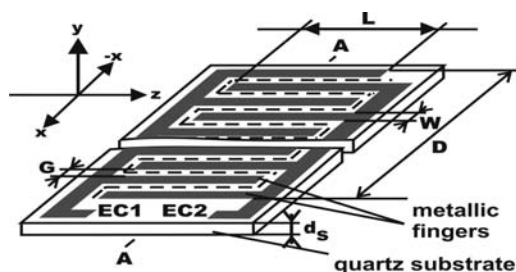
(EC1,EC2)-electric contacts

– – – – – · meander length

d_s - substrate thickness

A÷A   cross-secsion

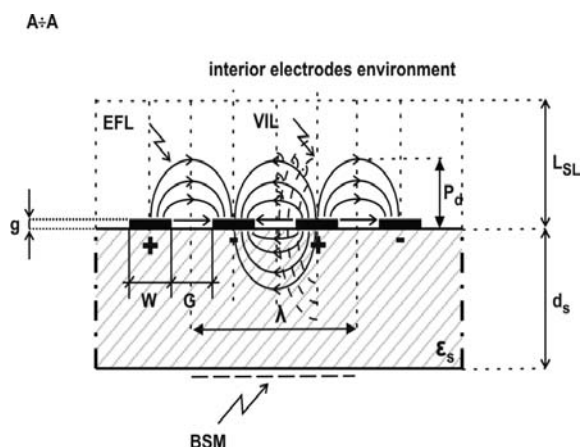Fig. 1. Schematic layout of interdigital capacitor (IDC) geometry and dimensions

A÷A

Fig. 2. Cross – section (A ÷ A) layout from Fig.1, with electric field strength lines and iso – lines of electric potential created by comb electrodes above the plain and within substrate material

Lower down, the specification of parameters of IDC used in the Fig. 1 and Fig. 2 are described.
W – metallic fingers width
G – inter fingers isolation gap width
EFL – electric field lines of forces
VIL – iso – lines of electric potential
L_{SL} – sensitive layer thickness
P_d – penetration depth of electric field
λ – spatial wavelength of periodic fingers system
g « w: flat electrodes approximation
ε_s – dielectric permittivity of substrate material
BSM – bottom substrate metallization (optional)
λ = W/(W+G) = 2W/ λ: metallization ratio of IDC

The most often value of W and G range from 1μm-100 μm and symmetrical configuration W = G is typical case in practice. Values of G and W define another parameter named metallization ratio of IDC, η. It is a measure of IDC surface covering step by metallic electrode. The whole electrode system of IDC creates a

standing electric field wave within the sensitive layer and substratum material. Sensitive layer region means the region in which material under test can be placed or simply dry air, semi infinite layer with dielectric permittivity ε (ε ≈ 1) – used for calibration purpose. In practice, IDC electrodes creates the effective measuring electric field penetrating materials under test into P_d range. For a given amplitude of generator amplitude P_d can be treated as depended rather on G and W values and will be specified later.

Spatial wavelength of periodic fingers system λ enables harmonic analysis of IDC properties and model but it will be subject of another, separate publication. At the moment, the reader can find this analysis in the literature [1].

3. Model of capacitance and electrostatic potential of IDC

The electrostatic approximation modelling for IDC was first solved by Engon [10]. The dynamic approach was introduce by Olthuis at all [11]. He introduced a method of determination of RC – time of IDC applied for fluid electrolyte conductivity. This method is useful in the estimation of switching frequencies in photosensors. Also the method of conformal mapping to describe the flat capacitor opening transformation in order to create the structure of 2 plates capacitor was applied [12]. Now, the selected outcomes of these above mentioned calculations will be presented.

In Fig. 3, two semi – infinite plots, whose edges are separated by G distance, and both charged as it is indicated therein. Calculations were made under approximation that thickness of both plates (metallic electrodes) is negligible as compared to their separation (G). The density of electric charge $\sigma_n(x)$ as well as $\sigma_p(x)$ (symmetry) is decaying down very fast along x increasing right to the +σ/2 and left from the – σ/2.
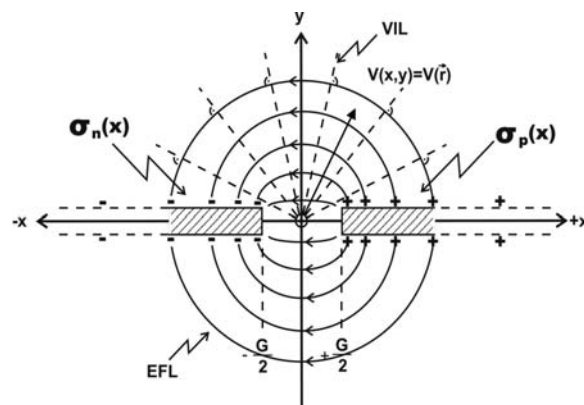

Fig. 3. Schematic representation of charge density distribution, field and potential iso-lines. It is meeded for V(x, y) as well as for σ(x) approximation in the case of internal IDC electrodes ($\sigma_n(x)$; $\sigma_p(x)$ – charge density distribution (total on both electrodes sides), other symbols as in the Fig. 2)

Thus, the electric field potential on the plane (y=0) and in the (x, y) plane can be approximated as [13]:

$$V(x, y) \approx \frac{2V_0}{\pi} \cdot \mathrm{Re}\left[\arcsin\left(\frac{x+iy}{G/2} \right) \right] \qquad (1)$$

where Vo is amplitude of applied measuring voltage.

Application of Gauss theorem, the surface charge density can be expressed as [14]:

$$\sigma_p(x) \approx -2\varepsilon \lim_{y \to 0}\left(\frac{\partial V(x, y)}{\partial y} \right) = -2\varepsilon \left(\frac{2V_0}{\pi} \right)\left(\frac{1}{\sqrt{\left(\frac{zx}{G} \right)^2 - 1}} \right)\left(\frac{2}{G} \right) \qquad (2)$$

The factor 2 in above equation is connected with the fact that plates with electric charge have 2 surfaces (Fig. 3). Because of symmetry reasons positive and negative charge densities must have the property

$$\sigma_n(x) = -\sigma_p(-x) \qquad (3)$$

The electric potential distribution V(x, y) is approximated as:

$$V(x, y) \approx \frac{4V_0}{\pi} \sum_{n=1}^{\infty}\left(\frac{1}{2n-1} \right) I0\left(\frac{(2n-1)\pi G}{G+W} \right) \times$$

$$\sin\left(\frac{(2n-1)\pi G}{2(G+W)} \right)\exp\left(-\frac{(2n-1)\pi |y|}{G+W} \right) \qquad (4)$$

where I_o – denotes zeroth Bessel function of the first kind, n – natural number

Above approximation can be applied for calculations without the need of using elliptic integrals as it is taking place in the conformal mapping procedure. For n = 1, the penetration depth P_d (into substrate and into material under test also) can be expressed as:

$$p_d \cong \frac{G+W}{\pi} \qquad (5)$$

Contribution of higher terms (n > 1) is small so equation (5) defines p_d quite good and p_d for example of MS-25 (Micromet/Netzsch) sensor equals about 16μm. Producer specifies value ~25μm for practical purposes. Thus, in the case of the metalization step ~ 50^0 and symmetry expressed by G = W, the P_d value is of G = W order.

Before the total capacity approximation, one have to integrate over the charge distribution as follows [14]:

$$Q \approx L \int_{G/2}^{(G/2)+W} \sigma(x)dx = -\lim_{y \to 0} 2\varepsilon L \int_{G/2}^{(G/2)+W} \frac{\partial V(x, y)}{\partial y} dx \qquad (6)$$

Thus, the total capacitance of IDC, after approximations can be expressed as:

$$C \cong LD\frac{4}{4(G+W)}\varepsilon\sum_{n=1}^{\infty}\left(\frac{1}{2n+1} \right)I_0^2\left(\frac{(2n-1)\pi G}{2(G+W)} \right) \qquad (7)$$

where L and D are defined in the Fig. 1.

It is worth to mention here, that analytical evaluation of charge, potential and capacity of IDC seems to be expressed mathematically as rather complicated one as compared to that of traditional flat or cylindrical capacitor. But from experimental point of view application of IDC is much simpler than that of flat or cylindrical one. Additionally, active surface of IDC can be very easy exposed into chemical vapours, liquids and electromagnetic radiation.

The total capacity (C) needed to evaluation of effective impedance (or admittance) of IDC in measurements of dielectric properties of materials under test.

4. Physical model of IDC

The equivalent circuit of IDC with RC elements representing the substrate capacity and resistance as well as material under test capacity with its resistance. There are two types of capacity and resistivity: external: C^e, R^e and internal one C^i, R^i. Total effective impedance can be calculated as parallel connection of two impedances:

$$\frac{1}{\hat{Z}_{ef}} = \frac{1}{\hat{Z}_{MUT}} + \frac{1}{\hat{Z}_{SU}} \qquad (8)$$

where:

$\hat{Z}_{ef}$ – effective impedance seen from electrical contacts

EC1 and EC2 measured by external meter LCR,

$\hat{Z}_{MUT}$ – impedance prescribed to material under test, representing the liquid, gas, solid layer or other form of the sample,

$\hat{Z}_{SU}$ – representing effective impedance of substrate caring metallic electrodes.

The $\hat{Z}_{MUT}$ can be calculated from equation (8) only if a appropriate conditions are valid:

1. Dielectric parameters of substrate ($\hat{Z}_{SU}$ = const.) is well established and known for the range of temperatures and frequency range applied in measurement.
2. The dielectric permittivity scale is calibrated for a given kind of measurement.

The condition nb.1 is fulfilled by selecting a very good and thermally stable substrate material with known dielectric permittivity value ε_s. Because the quartz is often used, the temperature range up 400 ^{0}C is in measurement rich.

What is important in practice, the total resistivity of substrate: $2R^e_{SU} + (N-2)R'_{SU}$ have to be much lower than thouse of material under test: $2R^e_{SL} + (N-2)R'_{SL}$. In practice 2 orders of magnitude difference makes the possibility of substrate reresistivity neglection. The condition nb.2 can be practically fulfield by measurement of equivalent capacity of "empty" IDC:

$$2\left(C^e_{SL} \right) + (N-2)\left(C^I_{SL} \right) + 2\left(C^e_{SU} \right) + (N-2)\left(C^I_{SU} \right) = C_1 \qquad (9)$$

N-2 segments/fingers

Legend:
e - external capacity/resitance
I - internal capacity/resitance
S - substrate
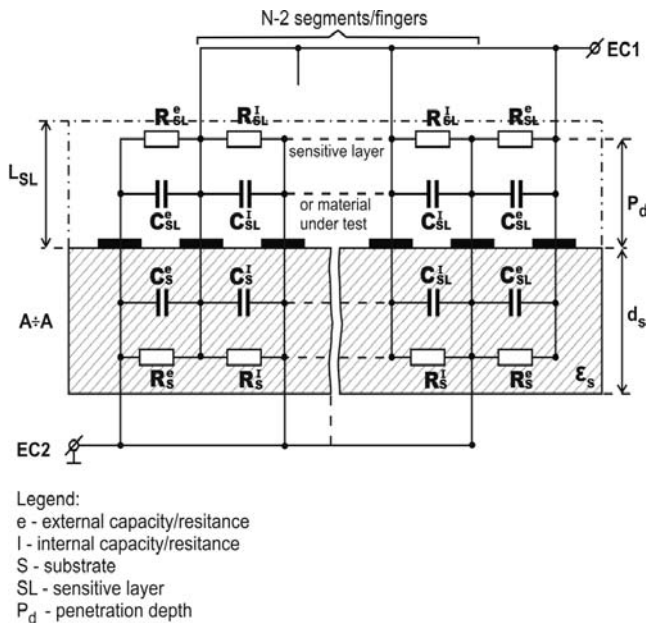SL - sensitive layer
P_d - penetration depth

Fig. 4. Equivalent circuit for total effective impedance measurement and calculation of IDC with material under test

In case when MUT is dry air, that $\varepsilon_{MUT} = 1.00$ and the first two components in equation (9) are connected with ε_{MUT} value. The 3-rd and 4-th components reflects the substrat dielectric permittivity ε_s; this one have to be determined by IDC producer. Thus we have the next relation:

$$C_{SL} + C_{SU} = C_1 \quad \text{and} \quad \frac{\varepsilon_{SU}}{\varepsilon_{MUT}} \cong \frac{C_{SU}}{C_{SL}} \tag{10}$$

for every frequency applied. Puting $\varepsilon_{MUT} \approx 1.00$ (dry air) one can calculate C_{sl} and C_{su} from (C_l; ε_{MUT}) values for each frequency. This can be done by PC program. The final test of calibration relayes on performing the measurement for selected points of frequency ω_i and checking wether in case of dry air (room conditions are enough) the flat line $\varepsilon_{MUT} \approx 1.00$ is drown by computer. In this way the effective material under test impedance Z_{MUT} can be calculated automaticaly as a function of frequency, the amplitude of electric voltage of measuring generator [4] and optionaly even dependence of this impedance on dc bias presence, temperature and so on. The physical model of $\hat{Z}_{MUT}(\omega)$ for a given MUT have to be created in every case of investigated material.

IDC can be also applied to investigate phase transitions in ferroelectric materials like those described formerly in [16] as well as piezoelectric properties typical for sensors and actuators design [17, 18].

References

[1] M.C. Zaretsky, L. Mouayed, J.M. Melcher, Continuum properties from interdigital electrode dielectrometry, IEEE Transactions on Electrical Insulation 23/6 (1988) 897-917.

[2] M.C. Zaretsky, J.R. Melchor, C.M. Cooke, Moisture sensing in transformer oil using thin-films microdielectrometry, IEEE Transactions on Electrical Insulation 24/6 (1989) 1167-1176.

[3] F. Starzyk, Interdigit dielectrometry of water vapour induced changes in granular starch, Archives of Materials Science and Engineering 29/1 (2008) 30–35.

[4] F. Starzyk, W. Bąk, C. Kajtoch, M. Gabryś, Influence of electric field DC-component on AC-response of ferroelectric powder, Archives of Materials Science and Engineering 29/1 (2008) 36-39.

[5] N.F. Shepard Jr, S.L. Garveric, D.R. Day, S.D. Senturia, Microdielectrometry: a new method for in situ cure monitoring, Proceedings of the 26th SAMPLE Symposium Los Angeles CA, 1981, 65-76.

[6] K.D. Haris, A. Huzinga, M.J. Brett, High-speed porous thin film humidity sensors, Electrochemical and Solid State Letters 5 (2002) H27-H29.

[7] W. On Ho, S. Krause, C.I. Mc Neil, Electrochemical sensor for measurement of urea and creatinine in serum based on ac impedance measurement of enzyme-catalyzed, polymer transformation, Analytical Chemistry 71 (1999) 1940-1946.

[8] U. Weimar, W. Goepel, Chemical imaging. Trends in practical multiparameter sensor systems, Sensor and Actuators B52 (1988) 143-161.

[9] R. Igreja, J.N. Morat-Mendes, C.J. Dias, Dielectric characterization of PEBA and POMS for capacitive interdigital vapour sensors, Proceedings of the 11th International Symposium on Electrets, Melbourne, Australia, 2002, 283-286.

[10] T. Schaefer, G. Bengtsem, H. Pingel, K.W. Boedeleker, J.P.S.G. Crespo, Recovery of aroma compounds from a wine-must fermentation by organofilic prevaporation, Biotechnology Bioengineering 62 (1999) 412-421.

[11] H. Engon, Interdigital electrode transducers for excitation of elastic surface waves in piezoelectric media, Internal raport no. TE-91, Institut for Teoretisk Elektroteknikk, Norwegian Institute of Technology, Trondheim, Norway.

[12] W. Olthuis, W. Streehstra, P. Bergveld, Theoretical and Experimental determination of cell constants of planed-interdigitated electrolyte conductivity sensors, Sensor and Actuators B24/25 (1995) 252-256.

[13] R. Igreja, C.J. Dias, Analytical evaluation of the interdigital electrodes capacitance for multi-layered structure, Sensor and Actuators A 112 (2004) 291-301.

[14] K.J. Biuns, P.J. Lawrenson, C.W. Trowbridge, The analytical and numerical solution of electric and magnetic fields, Wiley, New York, 1992.

[15] M.W. den Otter, Approximate expressions for capacitance and electrostatic potential of interdigitated electrodes, Sensor and Actuators A 96 (2002) 140-144.

[16] C. Kajtoch, W. Bąk, F. Starzyk, M. Gabryś, Study of phase transition specific in polycrystalline $Pb(Cd_{1/3}Nb_{1/3})O_3$, Archives of Materials Science and Engineering 29/1 (2008) 20-23.

[17] A. Buchacz, Influence of piezoelectric on characteristics of vibrating mechatronical system, Journal of Achievements in Materials and Manufacturing Engineering 17 (2006) 229-232.

[18] W. Bąk, F. Starzyk, C. Kajtoch, E. Nogas-Ćwikiel, Elevated temperature induced dispersion phenomena in $Ba_{1x}Na_xTi_{1-x}Nb_xO_3$, Archives of Materials Science and Engineering 29/1 (2008) 5-9.